Simulation Results of the Capacity of Cellular Systems

Zygmunt J. Haas, *Senior Member, IEEE,* Jack H. Winters, *Fellow, IEEE,* and David S. Johnson

Abstract— In this paper, we study the capacity of cellular systems with interference-adaptation dynamic channel allocation (DCA) through a set of heuristics that evaluate the required number of channels for some mobile traffic pattern. In particular, we evaluate the improvement in the reuse factor given the knowledge of the mobiles' locations. Assuming that the mobiles' locations are sampled from the uniform random distribution or are fixed on a uniform grid, we show the effect of a number of parameters, such as the number of mobiles per cell, the minimum allowable signal-to-interference ratio, and the limited knowledge of mobiles' locations. We also investigate the effect of shadow fading and signal-based power control. Although previous papers have proposed various heuristics with varying performance, here we present heuristics that are shown to give the maximum packing results based on our assumptions. In particular, the single-interferer assumption, used throughout our work, is justified and the optimality of the square-root signal-based power control is proven.

Index Terms— Dynamic channel assignment, fixed channel allocation, graph coloring, heuristics, interference cancellation, interference-adaptation dynamic channel allocation.

I. INTRODUCTION

A LARGE body of research has been published on the performance of cellular systems (e.g., [1]–[6]). Most of these papers present and analyze schemes in which no knowledge about the mobiles' precise locations (besides the cell in which the mobile currently resides) is taken into the account. Thus, a channel is allocated to a cell, rather than to a mobile. In this work, we assume that there is a mechanism by which mobiles can measure the amount of interference that they receive on different channels. Therefore, in our work, the allocation of channels is to mobiles rather than to cells. We show the amount of improvement that such a scheme carries.

In fixed channel allocation (FCA), a channel assigned to a cell can be reused according to some (fixed) cell reuse pattern ([1]). For example for cell reuse pattern of seven, the distance between cochannel base stations is about 4.6 cell radii. Similarly, for cell reuse pattern of three, the corresponding distance is three radii.

Because, at any time, some cells may require more capacity than others (i.e., the "hot spots" problem), the FCA suffers

from inefficient use of the radio spectrum. To correct this limitation of FCA, dynamic channel allocation (DCA) schemes have been proposed.[1] In fact, a multiplicity of DCA schemes have been investigated by various researchers, showing the advantage of one scheme over another under some traffic patterns and other assumptions (e.g., [7]–[11]). The traffic-adaptation-based DCA schemes rely on the idea that instead of dedicating the channels to cells, channels are placed in a pool and allocated on demand to the cells based on some allocation rules. Reuse of previously allocated channels is governed by the same minimal distance rule; i.e., a channel will not be reallocated in any cell that is closer than some minimal distance to another cell which was previously allocated by the same channel.

In both FCA and the traffic-adaptation DCA, the channels are usually allocated to cells based on the assumption that a mobile may be located anywhere within the boundary of that cell. Thus, for both the schemes, the "packing"[2] of channels is not maximal. These schemes suffer from the fact that the fixed reusability factor may be too pessimistic; e.g., mobiles that are close to their base stations may not interfere with each other even if they are in adjacent cells. In the interference-adaptation DCA schemes, mobiles measure the amount of interference to determine the usability of a channel. An example of a system based on this principle is the DECT standard ([12]). Such algorithms can, in principle, achieve maximal packing, but none have been shown to provide maximal packing in all cases. Indeed, the performance with maximal packing is not known. However, here we present heuristics, which are shown to closely approximate the number of required channels with maximal packing.

The number of channels required to support a given distribution of mobiles in each cell with the maximum packing strategy is termed by us the number of required channels N_c. For any channel allocation strategy and for the same mobile distribution, at least the N_c channels must be allocated to provide connection to all the mobiles. In other words, the number of channels with maximum packing is a lower bound on the number of channels required in any cellular system.

The N_c depends on a specific mobiles' configuration. Thus, N_c is a static measure. In other words, when the mobiles move, the particular assignment may not be valid anymore and may

<hr>

[1] We distinguish here between DCA schemes that respond to traffic changes (traffic adaptation) and to changes in the level of measured interference (interference adaptation). This terminology is borrowed from [6].

[2] Channel "packing" refers to the areas where a channel cannot be reused and how closely these areas are spaced.

need to be recomputed. This may lead to reassignment of the channels of many (if not all) of the mobiles in the system. We will investigate the effect of mobility on the required reassignment frequency.

In general, the N_c varies with the location of the mobiles. However, our results show that with randomly located mobiles (the random locations drawn from the uniform distribution), the variation in the N_c for different realizations of the random locations is relatively small. Therefore, we use Monte Carlo simulation to determine the N_c for a number of realizations and use these results to obtain an estimated value. This value corresponds to the required number of channels to achieve small probability of call blocking. In practice, we may not need to assign channels to all mobiles, but can block some small percentage of arriving calls. Here, we ignore this fact, which would result in somewhat fewer channels being required. Therefore, our results are somewhat conservative.

Also, because of the time variations in the traffic, the required number of channels will also vary in time. Using the results presented here and knowing the traffic variations (or distribution), one may readily determine the distribution of the required number of channels with the traffic variations.

This paper is organized as follows: in the next section, we describe the model of the cellular network and list the major assumptions used throughout this work. In Section III, we show the effect of the different parameters on the results of the maximum packing strategy. For example, we consider the effect of channel allocation based on the distance of the mobiles from their base station, without knowledge of the actual location of the mobiles. In Section III-G, we provide justification for the single-interferer assumption. The effects of shadow fading and power control are further investigated in Section IV. Finally, in Section V, we summarize and conclude the study. Two Appendixes are included at the end of the paper. Appendix A explains in details the procedures used to find the N_c. The optimality of the square-root signal-based power control is proven in Appendix B.

II. ASSUMPTIONS, PARAMETERS, AND METHODOLOGY

The following model is used throughout this work, unless specifically indicated otherwise.

1) The cellular structure is composed of 33 internal cells, as shown in Fig. 1, surrounded by additional cells. The purpose of the additional cells is to eliminate the "boundary effects," which would lead to too optimistic results (too small number of required channels). A base station is located in the middle of each cell, and serves the mobiles that are located within the boundaries of the cell. More precisely, the mobile/base-station association is based on the received signal strength; i.e., the base station allocated to a mobile is the one which received the strongest mobile's signal.

2) Except for Section III-D, the mobiles are randomly distributed within each cell. The number of mobiles per cell is a parameter in our study.

3) The *single-interferer* assumption: in our study we assume that there is only one interfering link (i.e., with the same assigned channel) to a communication link under study. In reality, there may be several other links communicating on the same channel and contributing interference to the link in question. However, as shown in Section III-G, when a single interferer is used to calculate channel allocation, there is only a small percentage of links with lower-than-designed-for signal-to-interference ratio (SIR). Thus, error in the N_c is small. Consequently, the *single-interferer* assumption is justified.

4) The up-link and down-link channels are paired; e.g., if a specific up-link channel is available for communication between a mobile and its base station, but its paired down-link channel suffers from too much interference, this pair cannot be used. Link pairing is common in many existing wireless air protocols (e.g., AMPS, IS-136, or GSM).

5) We initially do not consider *shadow fading*; our initial model accounts for Rayleigh fading and propagation loss only. Shadow fading is further investigated in Section IV.

6) Both the base stations and the mobiles are equipped with omnidirectional antennas.

7) Except for Section III-E, there is no power control at the mobiles or at the base stations. Power control is further investigated in Section IV.

8) We assume that adjacent channel interference is much smaller than the cochannel interference. Consequently, we neglect the former.

The parameters used in the study are the following:

n number of mobiles in each cell;

c total number of cells;

N total number of mobiles $(= n \cdot c)$;

α *interference radius*—the ratio between the distance from the base station to the interferer and the distance from the base station to the mobile in question;

P_{BS} power transmitted by a base station without power control (we assume all the base stations transmit the same power level);

P_M power transmitted by a mobile without power control (we assume all the mobiles transmit the same power level);

S received signal power;

I received interference power;

r exponent of radio signal propagation loss ($r = 2$ for free-space propagation for mobile radio $r = 3.8$ is usually assumed);

N_c number of channels required to accommodate the N users under given conditions;

x distance of a mobile to its base station;

d distance of a mobile to another base station (other than its own base station).

The study evaluates the minimal number of required channels,[3] referred to here also as colors, assigned to all the mobiles under given operating conditions, such that given interference conditions are satisfied. The operating conditions refer to the
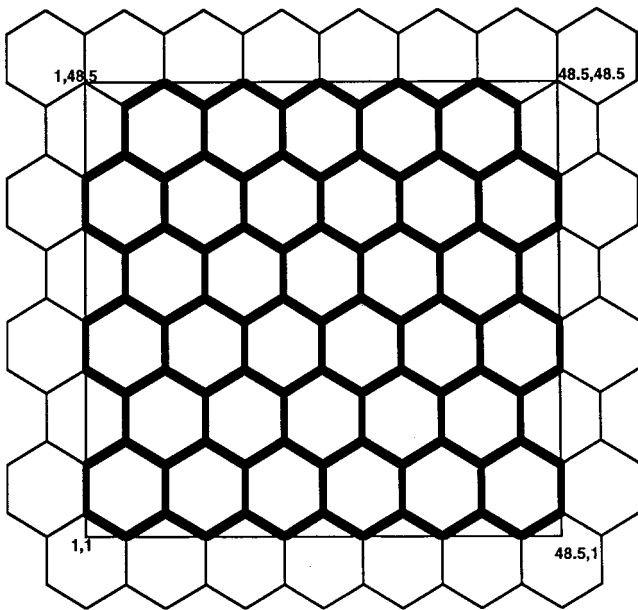
---

[3] I.e., maximal packing strategy.

Fig. 1. Cells structure.

knowledge or lack of knowledge of the location of the mobiles. The interference conditions refer to the acceptable level of interference, so that two mobiles can be assigned the same channel.

In this work, we consider FDMA/TDMA assignment. Two different TDMA slots are considered as separate channels and we assume here that such two channels do not suffer from cross interference; i.e., there is enough time guard between adjacent time slots.

The number of channels is evaluated by constructing a matrix (referred to here as the *compatibility matrix* of dimension $N \times N$); i.e., each mobile in the whole system is confronted with each other mobile to determine whether the two mobiles can be assigned the same channel (i.e., whether they are *compatible*) based on the interference conditions. A graph G is then composed, where each mobile in the system corresponds to a vertex in G. Two vertices are interconnected by an edge in the graph, if and only if the two mobiles represented by the two vertices are incompatible; i.e., they cannot be assigned the same channel. A set of graph coloring algorithms is then employed to find the minimum number of colors to color the vertices in the graph G, such that no two vertices interconnected by an edge are colored in the same color. Each color corresponds to a channel assigned to the mobiles that are colored in this color. (This problem can also be posed as finding the minimum number of cliques[4] that cover all the vertices in the complementary graph.[5] A clique in the complementary graph, then, corresponds to a channel.)

Theorem: The number of colors equals the minimum number of channels required to satisfy the compatibility relations between mobiles.

Proof: Assume that there is an assignment that satisfies the compatibility relations but with less channels than the

[4] A *clique* is a fully connected subgraph.
[5] The complementary graph is a graph with an edge between two nodes if and only if the nodes are not connected in the original graph.

number of colors from the graph coloring algorithm. Then, by assigning a different color to every channel, we found a graph coloring with less colors than the graph coloring algorithm, which contradicts the optimality of the graph coloring algorithm. □

For a small number of vertices, finding the number of colors may not be a considerable challenge. However, to obtain any meaningful statistics, instances with a large number of mobiles need to be evaluated. Thus, since the graph coloring problem is an NP-complete problem ([13]), finding the number of colors can be a complex task, as is the problem of finding the minimum number of cliques. In this work, we thus use an algorithm suggested by [14] that, while not finding the exact number of colors required, is remarkably effective at finding good upper bounds on that number for the types of graphs we create. We then employ heuristics to determine the maximum clique size on the graph G.[6] As proved in the following Theorem, the maximum clique size is the minimum number of required colors to color the graph. Consequently, the maximum clique size determines the minimum number of channels required and constitutes a lower bound on N_c. Having a lower and the upper bounds on N_c, allows us to pin the precise value to within a narrow range, and indeed often determining it exactly. In this respect, our work differs from others, who have proposed various heuristics, but have not shown if these are optimal, or even what the performance of these heuristics would be. Appendix A provides an extensive discussion of the heuristics used in this study.

Theorem: The maximum clique size corresponds to the minimum number of required colors to color the compatibility graph.

Proof: Assume that there is an assignment that colors the graph with less colors. Thus, there will be at least two nodes in the maximum-sized clique colored with the same color. But, this would contradict the construction of G; i.e., an edge in G connect two *incompatible* nodes that cannot be colored with the same color. Thus, one must use at least the number of colors equal to the maximum clique size. □

Other approaches to cope with the large complexity of the problem have been proposed. In particular, simulated annealing and neural networks were used ([15], [16]). Our algorithm is significantly faster than the simulated annealing and neural-net approaches and finds bounds that are typically just as good, or, in the latter case, significantly better. Moreover, such schemes usually suffer from the uncertainty whether the obtained solution is, in fact, optimal and how far is the obtained value from the optimal solution. Our "brute force" scheme presented here provides either an exact solution or tight bounds within which the optimal result exists.

Previous papers (e.g., [17]) have proposed various heuristics with varying performance. Our heuristics presented here are shown to give the maximum packing results based on our assumptions. In this sense, our work follows the results of these papers. Furthermore, the procedure for "bounding" the minimum number of channels based on the two sets of heuristics is the main contribution of this paper. (For example,

[6] Again, since the maximum clique problem is also an NP-complete problem, we utilize heuristics in our solution.

in [6], the FCA is compared with an interference-adaptation DCA scheme, with the results shown as two quite loose bounds.) The assumptions used in our work include the single-interferer assumption (see Section III-G) and the square-root power control, which is proven in Appendix B to be the optimal signal-based power control algorithm.

A. The Interference Conditions

In general, the SIR determines the ability of a receiver to recover the signal of power S in the presence of interference of power I. We assume that there is some minimum SIR, termed $\text{SIR}_{\min}$, required for satisfactory system operation.[7] Thus, in a system in which the desired signal of power P is transmitted from a distance x and the interference signal of the same power is transmitted from a distance d, the SIR is

$$\text{SIR} = \frac{S}{I} = \frac{\frac{P}{x^r}}{\frac{P}{d^r}} = \left(\frac{d}{x}\right)^r \geq \text{SIR}_{\min}. \tag{1}$$

We define α to be

$$\alpha = \sqrt[r]{\text{SIR}_{\min}}. \tag{2}$$

Thus, to achieve sufficient performance (i.e., $\text{SIR} \geq \text{SIR}_{\min}$)

$$\frac{d}{x} \geq \alpha. \tag{3}$$

Assume two mobiles, one in each cell, as shown in Fig. 2. If the two mobiles are assigned the same up link channel and the two base stations are assigned the same down link channel, then the SIR of the link between the base station$_A$ and the mobile A, resulting from the interfering communication between the base station$_B$ and the mobile B is

$$\text{SIR}_A = \frac{\frac{P_{\text{BS}}}{(x_A)^r}}{\frac{P_{\text{BS}}}{(d_A)^r}} = \left(\frac{d_A}{x_A}\right)^r \tag{4}$$

and the SIR of the link between the mobile A and the base station$_A$, resulting from the interfering communication between the mobile B and the base station$_B$ is

$$\text{SIR}_{\text{BS}_A} = \frac{\frac{P_M}{(x_A)^r}}{\frac{P_M}{(d_B)^r}} = \left(\frac{d_B}{x_A}\right)^r. \tag{5}$$

Similarly

$$\text{SIR}_B = \frac{\frac{P_{\text{BS}}}{(x_B)^r}}{\frac{P_{\text{BS}}}{(d_B)^r}} = \left(\frac{d_B}{x_B}\right)^r \tag{6}$$

$$\text{SIR}_{\text{BS}_B} = \frac{\frac{P_M}{(x_B)^r}}{\frac{P_M}{(d_A)^r}} = \left(\frac{d_A}{x_B}\right)^r. \tag{7}$$

Since each one of the SIR's must satisfy the condition that $\text{SIR} \geq \text{SIR}_{\min}$, (4)–(7) correspond to the following set of conditions:

$$\begin{aligned} d_A &\geq \alpha \cdot x_A & d_B &\geq \alpha \cdot x_A \\ d_B &\geq \alpha \cdot x_B & d_A &\geq \alpha \cdot x_B. \end{aligned} \tag{8}$$

---

[7] The $\text{SIR}_{\min}$ is determined for a data transmission system by the required raw bit-error rate and for a voice communication system by a subjective intelligibility test.
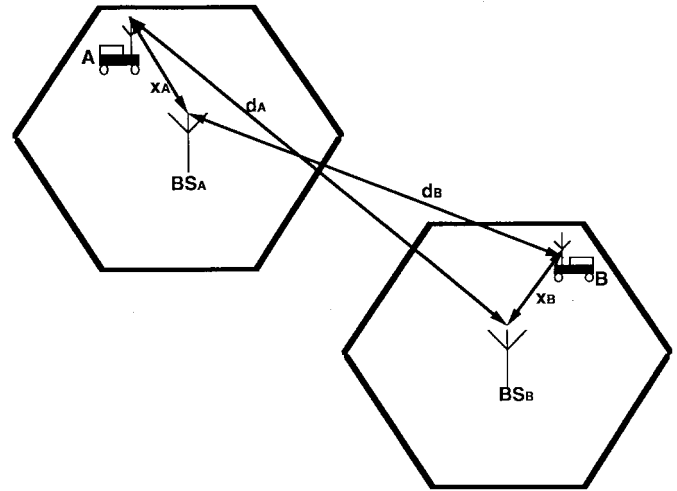

Fig. 2. Interference distances.

In our simulation, we randomly distribute n mobiles throughout the area of each cell, with the random location drawn from the uniform distribution. The conditions (8) are checked for every pair of mobiles and two mobiles are declared compatible if the conditions (8) are satisfied. Otherwise, the mobiles are incompatible. The results are arranged in the compatibility matrix, which is used as an input to our graph-coloring and clique finding algorithms. From these algorithms we obtain the upper and the lower bounds (typically quite tight) on the N_c required to support communication to/from all the mobiles in the specific mobiles' constellation and with SIR greater than $\text{SIR}_{\min}$. We ran the simulation large enough number of times, so that $\pm 5\%$ of the estimated value of N_c represents a 95% confidence interval. Typically, as long as we do not consider the shadowing and power control effects, the distribution of the results from various simulation runs is quite small.

While knowing the location of each mobile may not be possible, all that is necessary for maximal packing is the knowledge of the signal levels of each mobile's signal at all the base stations and the knowledge of each base-station signal at all the mobiles. With such knowledge, any two nodes can be confronted to determine their compatibility status by calculating the SIR for such channel allocation. Such a scheme may be used for an implementation of the algorithms described here in a practical system.

III. ESTIMATION OF THE NUMBER OF REQUIRED CHANNELS

In this section, we show the effect of the various parameters in our system on the number of required channels, N_c.

A. The Effect of the Number of Mobiles per Cell

The number of required channels, N_c, as a function of mobile density is shown in Fig. 3 and was evaluated for the following number of mobiles per cell: $n = 1$, 2, 4, 8, 15, 30, 45, 60, 90, and 120. As demonstrated in this figure, the number of channels increases linearly with the mobile density, measured here in mobiles-per-cell. The results shown in this figure were obtained with $\alpha = 2.0$, which corresponds
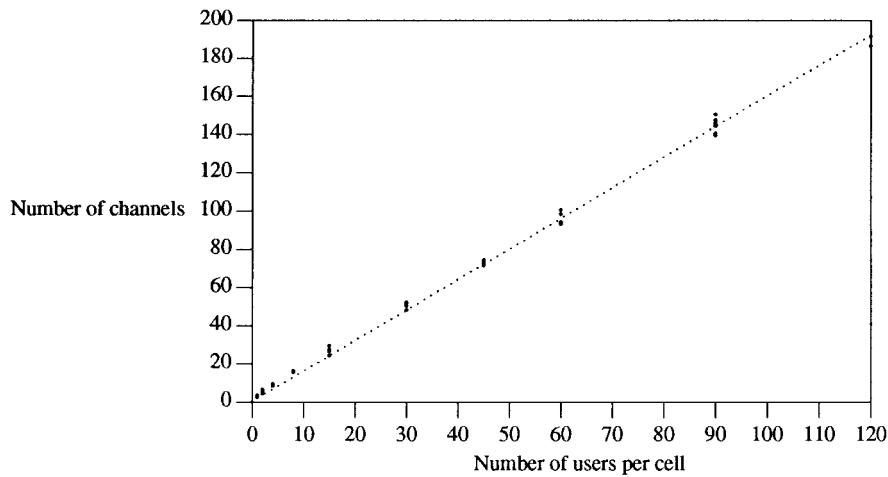
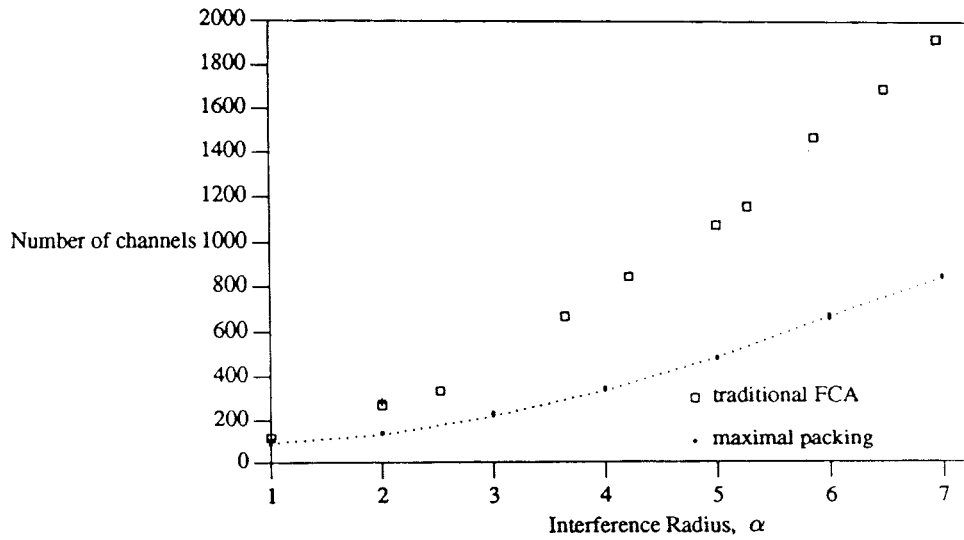Fig. 3. Number of channels as a function of mobile density.

Fig. 4. Number of channels as a function of the interference radius.

to reuse pattern of three. The slope of the curve in Fig. 3 is about 1.6. Thus, we have shown that for $\alpha = 2$, the reduction in the number of channels offered by maximal packing, as opposed to the fixed reuse pattern, is approximately the factor of two; i.e., the maximal packing requires only about half as many channels as FCA. Because of the linear behavior, many of our results that follow are independent of the actual number of mobiles per cell.

B. The Effect of the Interference Radius

The two curves in Fig. 4 show the dependence of the number of required channels on the interference radius α for the maximal packing scheme. The results were obtained for 90 mobiles per cell.

For comparison purposes, the traditional FCA scheme is also shown in the above figure. The number of channels for the traditional scheme was obtained by the following formula (taken from [7] with adjustments to reflect our definitions):

$$N_c(\text{FCA}) = \frac{n}{3}(\alpha + 1)^2. \tag{9}$$

Note that the above formula is valid at specific discrete values of the reuse factor. These values were translated to the corresponding values of α, as indicated in Fig. 4.

As clearly shown in the figure, the actual gain achieved by the maximal packing algorithm increases with the interference radius as compared with the traditional FCA. For example, at $\alpha = 2$ and at $\alpha = 3.6$, the traditional FCA requires 270 and 630 channels,[8] respectively, and approximately 145 and 230 channels, respectively, for the maximum packing scheme. Thus, the improvement consists of 46% and 63% reduction in the required number of channels, respectively.

C. The Effect of No Knowledge of Direction (Azimuth)

By measuring the received power,[9] the base station may be able to determine the equivalent distance of the mobile, without knowing its actual position; i.e., operation with ig-

---

[8] For the interference radii of 2 and 3.6, the corresponding reuse patterns for the traditional FCA are 3 and 7, respectively.

[9] When power control is performed, additional information on the transmitted power needs to be conveyed to the receiver site.
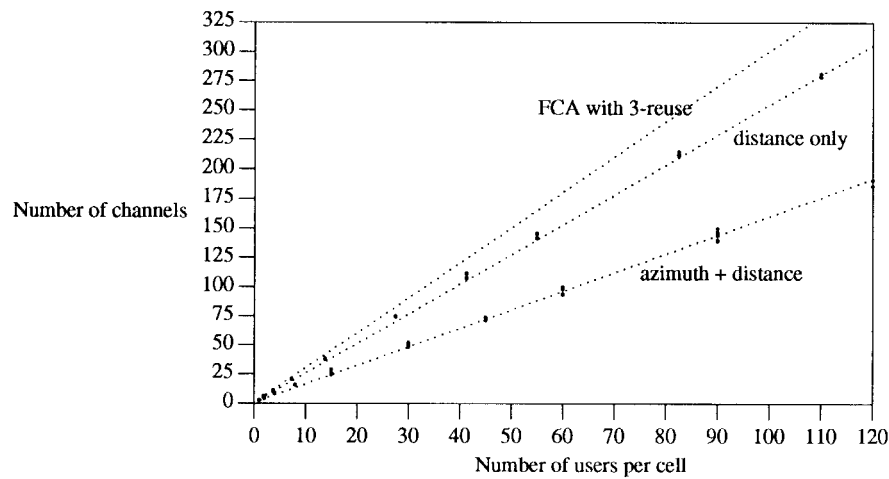
Fig. 5. Number of channels as a function of mobile density when the azimuth is not known.
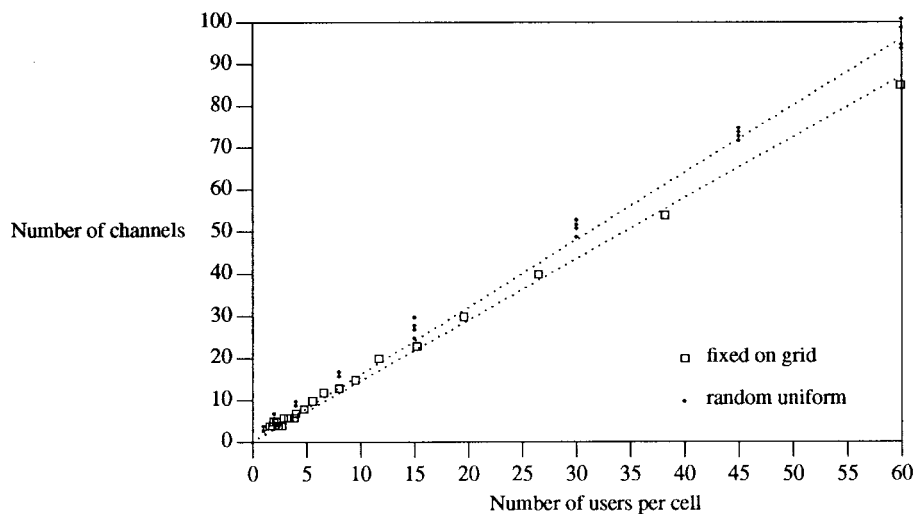

Fig. 6. Number of channels as a function of mobile density for uniformly distributed mobiles.

norance of the azimuth value. When the maximum packing is performed without the knowledge of the azimuth, the gain of the maximum packing is reduced, as shown in Fig. 5. The curves "azimuth + distance" and "distance only" represent the cases when the actual location of the mobile is known, and when only the distance of the mobile from the base station is known, respectively. For comparison purposes, the curve "FCA with three reuse" shows the results for the traditional FCA with a reuse pattern of three. Results in Fig. 5 were obtained with $\alpha = 2.0$. Thus, for example, for 90 mobiles per cell and for $\alpha = 2.0$, the number of required channels with no knowledge of direction is 229, or a reduction of 15% only from the 270 channels required for the traditional FCA scheme. This is about a third of the 46% reduction, when both the direction and the azimuth are known (i.e., from 270 to 145 channels).

D. The Effect of Mobile Distribution Within the Cell

The previous results were obtained by assuming random (uniform) distribution of mobiles within a cell. When the mobiles' locations are fixed on a uniform grid, the gain of the maximum packing algorithm is considerably improved, since regions of high mobile concentration ("hot spots") can occur under the random distribution. Obviously, such regions are not present in the fixed uniform distribution case, and the results are shown in Fig. 6. As shown in this figure, the slope of the curve is about 1.4, indicating about 15% fewer channels than in the randomly distributed case. The results were obtained with $\alpha = 2.0$. The actual position of the grid with respect to the cellular structure has no noticeable effect with large number of mobiles per cell.

E. The Effect of Full Power Control

In this section, we show that full signal-based power control has no effect on the number of channels, as investigated in this study.

In a signal-based power-controlled environment, mobiles transmit their signal with dynamically adjusted power level, so that a constant power level is received at the base stations; i.e., the effect of loss and fading is compensated for. Similarly, the power of base stations' transmission is adjusted, so that the signal received at the mobiles is of constant level.

If the power received by a mobile is P_{BS}, the actual power transmitted by a base station located at a distance x is $P_{\mathrm{BS}} \cdot x^r$. Similarly, if the power received by a base station from a mobile located at a distance x is P_M, the mobile needs to transmit power of $P_M \cdot x^r$. Consequently, (4)–(7) can be rewritten as

$$\mathrm{SIR}_A = \frac{\frac{P_{\mathrm{BS}} \cdot (x_A)^r}{(x_A)^r}}{\frac{P_{\mathrm{BS}} \cdot (x_B)^r}{(d_A)^r}} = \left(\frac{d_A}{x_B}\right)^r \tag{10}$$

$$\mathrm{SIR}_{\mathrm{BS}_A} = \frac{\frac{P_M \cdot (x_A)^r}{(x_A)^r}}{\frac{P_M \cdot (x_B)^r}{(d_B)^r}} = \left(\frac{d_B}{x_B}\right)^r \tag{11}$$

$$\mathrm{SIR}_B = \frac{\frac{P_{\mathrm{BS}} \cdot (x_B)^r}{(x_B)^r}}{\frac{P_{\mathrm{BS}} \cdot (x_A)^r}{(d_B)^r}} = \left(\frac{d_B}{x_A}\right)^r \tag{12}$$

$$\mathrm{SIR}_{\mathrm{BS}_B} = \frac{\frac{P_M \cdot (x_B)^r}{(x_B)^r}}{\frac{P_M \cdot (x_A)^r}{(d_A)^r}} = \left(\frac{d_A}{x_A}\right)^r. \tag{13}$$

Thus, the four conditions that the locations of the two mobiles need to fulfill to be assigned the same channel (i.e., to be compatible) are

$$\begin{aligned} d_A \geq \alpha \cdot x_B \quad & d_B \geq \alpha \cdot x_B \\ d_B \geq \alpha \cdot x_A \quad & d_A \geq \alpha \cdot x_A \end{aligned} \tag{14}$$

which are exactly the conditions (8) in different order. Thus, we conclude that two mobiles' locations are compatible, regardless of whether full signal-based power control is performed or not; i.e., our results are applicable to both the power-controlled and the noncontrolled cases. A similar conclusion can be drawn from [18].

F. A Practical Assignment Policy

As noted in Section II-A, for the implementation of the maximum packing scheme, knowledge of the actual distances between the mobiles and their base stations are not necessary. Instead, the received power levels at the mobiles and at the base stations suffice. However, since in the maximum packing scheme described in this paper channels are assigned to mobiles (and not cells) and the assignments are based on the mobiles' locations, the optimal (or even a feasible) assignment may change as the mobiles move throughout the coverage area. This may lead to a large number of channel reassignments, too large for a practical implementation. In this section, we present a scheme that trades off the number of reassignments with the reuse factor (i.e., number of required channels). This is done by dividing the cells into smaller areas, termed here *subcells*. Fig. 7 shows an example of such an arrangement. The resolution of mobiles' locations is now reduced to a subcell; i.e., a base station's knowledge of a mobile location is limited to the identity of the subcell. No reassignment will take place as long as a mobile does not leave the subcell area—thus, the number of reassignments is reduced. However, because there is no knowledge of the actual location of mobiles within the subcells, a channel assigned to a mobile must now be reused at a larger distance than before. Thus, the reuse factor is reduced. Here, we estimate
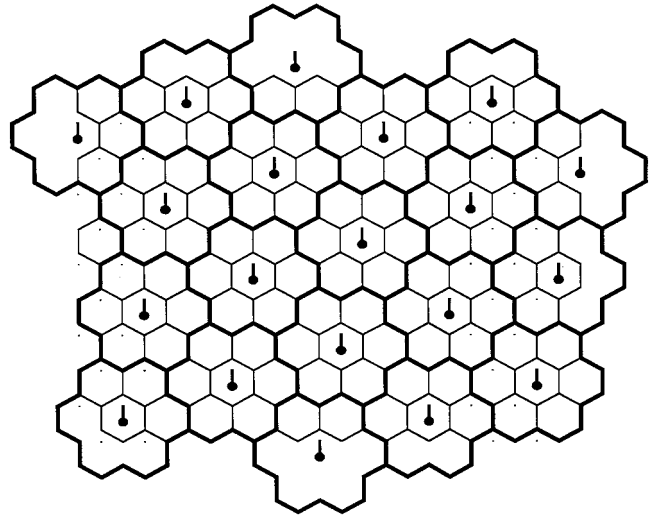

Fig. 7. Cells and subcells.

this reduction, showing that when the number of subcells per cell is larger than about 20, the reduction in the reuse factor is relatively small.

To evaluate the number of channels required to support 90 users per cell with $\alpha = 2.0$, a uniform grid was superimposed on the hexagonal structure bounded by the rectangular area in Fig. 1. The spacing of the uniform grid was kept as a parameter. Each point on the grid represents a center of a subcell. Each subcell was associated with a base station by determining the shortest distance between the center of the subcell and all the base stations.[10] A mobile was then placed in each subcell and the number of required channels was evaluated. This number was then scaled up to allow 90 mobiles per cell. The interference evaluation assumed worst case conditions; i.e., that the mobile and the interferer are on the circumference of their subcells, with the interferer being closest to the mobile's base station and the mobile being furthest away from the base station.

The results are plotted in Fig. 8. Note the relatively large number of channels required when there is a small number of subcells per cell. This is because in the investigated scheme, only the center of the subcell determines the base station that this subcell is associated with. For large subcells, a considerable portion of the subcell can be closer to a base station other than the one it was actually associated with, resulting in a considerable loss of performance. (This phenomenon can be avoided, if a structure similar to the one shown in Fig. 7 is used. Nevertheless, the effect of this phenomenon is relatively small for the large number of subcells per cell, which is the case of interest here.) As can be observed from Fig. 8, when the number of subcells per cell exceeds 20, the degradation due to the subcell structure is relatively small (i.e., about 150 channels, compared with about 145 channels needed when the maximum packing scheme with no subcell structure is used, as in Fig. 3).

---

[10] Such assignments of subcells to cells may result in unequal number of subcells per cell. However, for large number of subcells, this phenomenon is negligible.
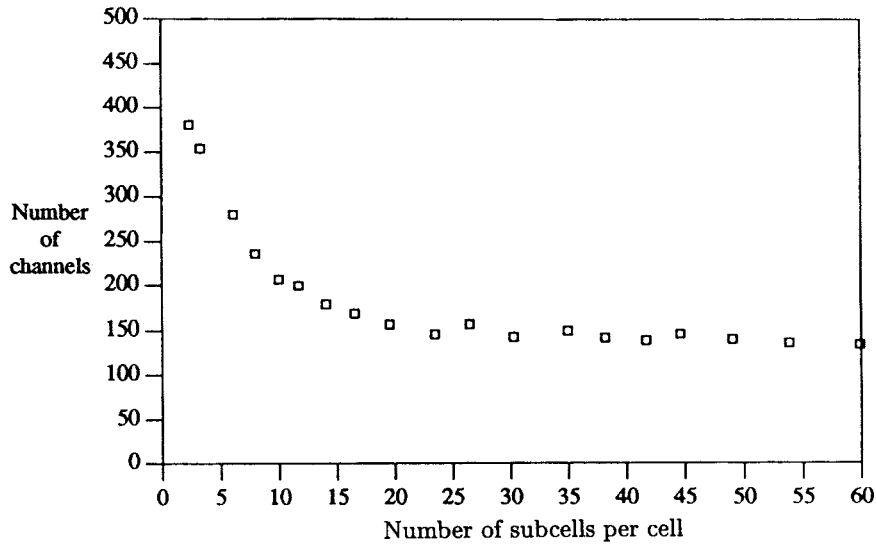
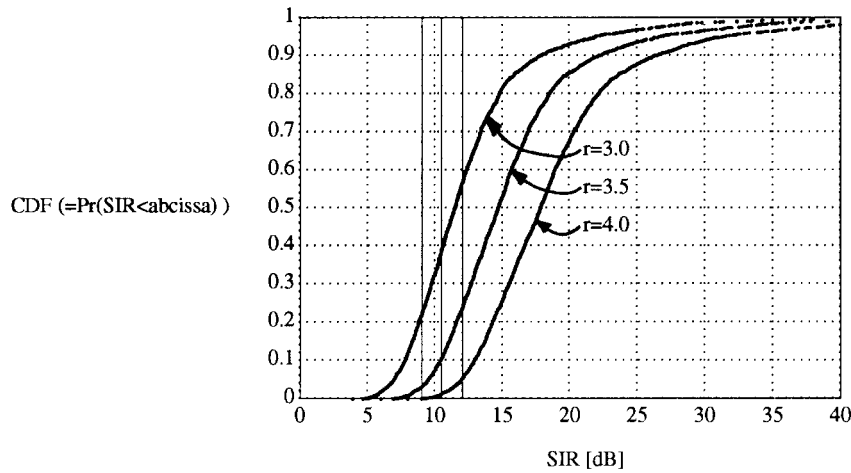Fig. 8.   Performance of the practical assignment scheme.

Fig. 9.   Cumulative probability distribution function of the mobiles' SIR.

G. The Effect of the "Single-Interferer" Assumption

Throughout this study, we have assumed a single interferer; i.e., in each case, there is one interferer that is significantly closer than all the other interferers. In this section, we justify this single-interferer assumption.

In Fig. 9, the probability distribution function of the mobiles' SIR is shown for the cases of $r = 3.0$, 3.5, and 4.0. The probability distribution was obtained for $\alpha = 2.0$ by analyzing the actual assignments generated by the graph-coloring algorithms. In other words, using the assignments obtained from the graph-coloring algorithm, the power levels of the interfering signals at each mobile from all the other mobiles (with the same assigned channel) were calculated. Then, the SIR for each mobile was obtained by dividing the computed signal power by the sum of all the interferers' power. The statistics of all the mobiles were obtained, resulting in the cumulative distribution function (CDF) in Fig. 9. For $\alpha = 2.0$, the corresponding $\text{SIR}_{\min}$-s for the above three values of r are 9, 10.5, and 12 dB, respectively. Vertical

lines corresponding to these values are shown in the Fig. 9. Considering all the interferers, Fig. 9 shows that, with the single-interferer assumption, the percentages of mobiles with SIR worse than $\text{SIR}_{\min}$ are: 20%, 10%, and 5%, for $r = 3.0$, 3.5, 4.0, respectively. Thus, the results generated using the single-interferer assumption contain channel assignments with relatively small percentage of mobiles violating the SIR that the system was originally designed for. If these mobiles with too low SIR were to be assigned channels, unused by the rest of the mobiles, the increase in the number of channels would then be at most 32%, 16%, and 8%, respectively.[11] Consequently, the error in the number of required channels, N_c, due to the single-interferer assumption for $r = 3.8$ is approximately 11% and may be considered negligible. Alternatively, one may adjust the results obtained here by increasing the estimated N_c by the above error factor.

[11] Of course, this is the worst case scenario. In practice, the mobiles with too low SIR may still be able to reuse some of the channels used by the other mobiles.

IV. EFFECTS OF SHADOW FADING AND POWER CONTROL

In this section, we present some results showing the effect of shadow fading and signal-based power control on the performance of the maximal packing scheme.

Shadow fading is modeled as a random variable (Θ) of lognormal distribution with $\sigma = 8$ dB and mean value corresponding to the propagation exponent of $r = 3.8$. (In the case where there is no shadow fading, the propagation loss exponent remains at $r = 3.8$.) It is assumed that the shadow fading is transmission-direction independent; i.e., its value for the up- and the down-links between two points is the same.

The signal-based power-control strategy is to partially compensate for the signal fading due to shadowing. We use square-root power control, which effectively reduces the loss (with or without the shadow fading) to half of their values in decibels. The square-root power control is proven in Appendix B to be optimal (see also [19] and [20]) for power control based on received signal strength alone. Note that better performance can be achieved with interference-adaptation power control, which could be used in combination with interference-adaptation DCA. However, heuristics for this case were not considered in this paper.

The results are shown in Fig. 10 for $n = 30$. The shadow fading affects the compatibility matrices, making them considerably less sparse. This causes larger range between the lower and the upper bounds, making it more difficult to draw definite conclusions. Nevertheless, Fig. 10 shows the improvement of the power control mechanism, both with and without the shadow fading. An interesting observation is that the shadow fading may actually reduce the number of required channels, especially for large α. This conclusion can be intuitively justified by observing that the *average* effective distance of mobiles to their corresponding base stations decreases when shadowing is present. The reason for this stems from the facts that shadowing is a zero-mean process (in decibels) and that, for the same radius incremental, the larger the radius is, the more mobiles there are.[12] Thus, the size of the zone in which a channel cannot be reused decreases; i.e., the number of interfering nodes decreases. This decrease is larger for larger α-s. Of course, this phenomenon is balanced by an opposite trend, in which the number of incompatible nodes increases due to a similar process of reduction in the average distance between the base station and other nodes. The net outcome is as shown in Fig. 10: at small α-s the shadowing increases the number of required channels, while at large α-s the opposite is true.

V. CONCLUDING REMARKS

In this paper, we have investigated the performance of the maximum packing algorithm for cellular structure, which use the interference-adaptation DCA. In particular, we have proposed a procedure based on two sets of heuristics, which allow estimating the number of channels required to serve a given mobile population.

Our results are innovative in the sense that the channel assignments are done based on the knowledge (or limited
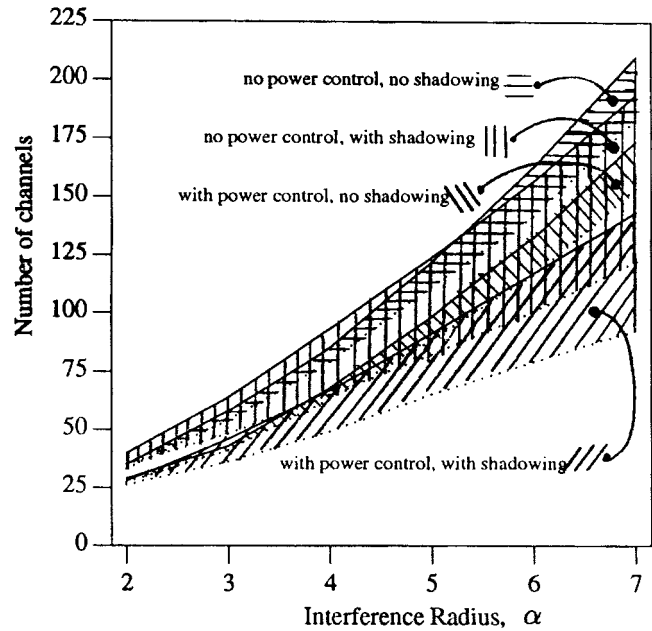

Fig. 10. The effects of shadow fading and power control.

knowledge) of the mobiles' locations. Thus, the cellular structure does not, by itself, limit the reuse of channels. An example of such a system is one in which the mobiles (and the base stations) measure the amount of interference to determine the available channels. The assignments are then done based on these measurement results.

Our proposed procedure used heuristics for graph-coloring and clique-finding problems to obtain estimates on the number of channels needed in each situation. The specific set of heuristics used for our implementation was chosen both for their speed and for the quality of results they yielded, and in these respects seemed to significantly outperform other methods such as simulated annealing and neural nets.

The results of this study indicate that the maximal packing scheme presented here can reduce the number of channels by nearly a factor of two, for an interference radius of 2.0. When only the distance (or power level) between each mobile and its nearest base station is known, the reduction in the number of channels is somewhat modest, 15% for interference radius of 2.0. More uniform mobile distribution reduces the number of required channels, since mobile clustering tends to reduce the channel reuse. We found about a 15% difference in the number of channels between the random (uniform) and the fixed (on a square grid) cases, for interference radius of 2.0.

We have demonstrated that full signal-based power control that compensates for the total propagation loss has no effect on the number of channels. Furthermore, we have proven that the optimal signal-based power control strategy is the square-root scheme. This is, by itself, an important result. We have also investigated the performance of the square-root power-control scheme, showing that the square-root power control reduces the number of channels by about 20% for $\alpha = 2$ and by more than 30% for $\alpha = 7$.

We have justified the single-interferer assumption used throughout our study, showing that it corresponds to a small

---

[12] The number of mobiles per area unit is constant.

11% error (for $r = 3.8$) in the number of required channels. Additionally, our results are also valid (with some minimal error) when a small amount of blocking is allowed in the system.

Finally, we have investigated the effect of the shadow fading phenomenon, surprisingly concluding that shadow fading may, in fact, reduce the required number of channels, especially for large interference radii. The observed degradation due to the shadow fading at small α-s is relatively minor.

The schemes shown here may be of particular interest to the emerging personal communication networks, based on microcellular infrastructures. In these systems, the user density is predicted to increase considerably and efficient spectrum reuse may be crucial for practical commercial attractiveness of such systems.

APPENDIX A
FINDING THE MINIMUM NUMBER OF COLORS

The problem of determining the minimum possible number of channel pairs for a given distributions of mobiles can be phrased as a graph coloring problem. One such problem had to be solved for each data point in Figs. 3–9 and 8. In this Appendix, we describe the solution techniques we used.

First some definitions. Given a graph $G = (V, E)$, where V is the set of vertices and E is the set of (undirected) edges, a k coloring of G is a partition of V into k sets $V_1, \cdots, V_k$ such that no two vertices in the same set V_i are *adjacent*, i.e., make up an edge in E. (We say that the vertices in set V_i are assigned "color i.") The *chromatic number*, $\chi(G)$, is the minimum integer k, such that G has a k coloring. Recall that in our application, the vertices represent mobiles, with an edge between two mobiles if they cannot use the same channel because of potential interference. By determining the chromatic number of G, we also determine the minimum possible number of channel pairs in an FDMA channel assignment.

Unfortunately, the problem of precisely determining the chromatic number is an NP-hard problem [13], and hence unlikely to be efficiently solvable in general. (The best general algorithms run in exponential time, and are typically unfeasible even for 100-vertex graphs, whereas most of the graphs we need to test have from 800 to 4320 vertices.) The approach we have thus taken is to use heuristics in an attempt to obtain tight upper and lower bounds on $\chi(G)$.

Relatively fast heuristics for finding "good" colorings (and hence upper bounds) have been proposed by a variety of authors, and many were implemented for use in a previous study [21]. We match these with lower bounds obtained by looking for large cliques in the graph. A *clique* in G is a subset $V' \subseteq V$ of the vertices such that for every pair of vertices u, v in V', $\{u, v\}$ is an edge of G. The size of the largest clique in a graph G is denoted by $\omega(G)$. Note that $\chi(G) \geq \omega(G)$, since every vertex in the maximum clique must be assigned a distinct color. The problem of computing $\omega(G)$ is also NP-hard, but here a version of a branch-and-bound algorithm suggested by [22] often can determine it in reasonable time for our smaller graphs and for our larger graphs a randomized search heuristic

to be described below has proved remarkably successful at obtaining good lower bounds.

Let us now briefly describe the algorithms we used, first for coloring and then for finding large cliques. For coloring, the workhorse of our computations was a variant on the algorithm *smallest-last with interchange* (SLI) first proposed by Matula *et al.* in [23]. That algorithm begins by reordering the vertices according to degree. Recall that the *degree* of a vertex in a graph is the number of edges of the graph that have that vertex as an endpoint. If V' is a subset of the vertices of $G = (V, E)$, the *subgraph induced by V'* is $G' = (V', E')$, where E' is the subset of E consisting of all those edges which have both endpoints in V'. Our new order $v_1, v_2, \cdots, v_n$ is constructed so that it has the following property: for each i, $1 \leq i \leq N = |V|$, v_i is a vertex of minimum degree in the subgraph of G induced by $v_1, \cdots, v_i$ (ties broken randomly). (Hence the name "smallest-last.") Such an ordering can easily be constructed in $O(|V|^2)$ time by working backward, starting with the choice of v_n.

We then color the vertices sequentially, starting with v_1. The first vertex v_1 is placed in color class V_1. Thereafter, when processing vertex v_i, we first determine whether there is some currently nonempty color class that contains no vertices adjacent to v_i. If so, we assign v_i to the lowest indexed class that has this property. Otherwise, we consider in turn each pair of nonempty color classes V_j and V_k, $j < k$ as follows. Let $G_{j,k}$ be the subgraph of G induced by $V_j \cup V_k$. Let N_j and N_k be the subsets of V_j and V_k, respectively, that are adjacent to our vertex v_i. Let C_j be the union of the connected components of $G_{j,k}$ that contain vertices of N_j, and let C_k be the union of the connected components of $G_{j,k}$ that contain vertices of N_k. (Recall that a connected component of a graph $G = (V, E)$ is a maximal subset $U \subseteq V$ such that if $u \in U$ and $\{u, v\} \in E$, then $v \in U$.) If C_j and C_k are disjoint, we perform an interchange of colors on C_j, moving all vertices in $C_j \cap V_j$ to V_k and all vertices in $C_j \cap V_k$ to V_j. It is easy to see that our interchange still yields a valid coloring of v_1 through v_{i-1}, but now v_i is no longer adjacent to any vertex in V_j, and so we can assign it to that class and go on to the coloring of v_{i+1}. If the above search for interchanges fails for all pairs of nonempty color classes, we start a new color class V_h, where h is one more than the maximum index of a currently nonempty color class, and assign v_i to V_h.

The above algorithm differs slightly from that of [23], which only considered pairs V_j, V_k for which $|N_j| = |N_k| = 1$. In practice, our version is significantly more effective without enduring a major increase in running time. (Both it and the original algorithm have worst case running time $O(|V||E|)$.) In general, it is not always as effective as such alternative approaches as simulated annealing [21] and tabu search [24], but for the graphs arising in our cellular application, it tends to give the best results, and to do so quickly. Because of the randomness involved in the initial reordering of the vertices, it can give different results from run to run. Typically we would run it on the order of 100 times on a graph and take the best result seen, which was often an optimal coloring.

We were able to confirm the optimality of many of our colorings because for many of the graphs we considered,

we were able to find a clique with as many vertices as the number of colors used in our best coloring. As mentioned above, we had two approaches to finding large cliques. The first was a branch-and-bound algorithm that determined the exact size $\omega(G)$ of the largest clique and is a close variant on the algorithm of [22]. The algorithm, which we shall call CMAX, assumes that the vertices are initially indexed in smallest-last order as described above, but beyond that proceeds recursively. Our global champion clique size M is initially one (any single vertex will do). We begin by setting our working clique C equal to the empty set and then treat the vertices in reverse order starting with v_n. For a given working clique C and vertex v, we call the algorithm recursively on the graph induced by the set of vertices with smaller indexes than v that are adjacent to all vertices in $C' = C \cup \{v\}$. If the maximum clique size M' returned is such that $M' + |C'| > M$ we update our global champion. The only pruning of subproblems that we do is based simply on cardinality. If the number of vertices in a generated problem is seen to be no greater than $M - |C'|$, that subproblem cannot yield a new champion and so we do not handle it (or even complete its generation, if we detect this in the middle of the generation process). Our code has a finely tuned inner loop. It is an inherently exponential-time algorithm and can be impractical even for relatively small graphs ($N = 200$) when the edge density (average vertex degree divided by N) is high. It has, however, run quickly for many of the graphs in this study, even some of those with as many as 2160 vertices.

When CMAX did not terminate within reasonable time bounds, or did not seem likely to do so, we reverted to a heuristic that uses CMAX as a subroutine in a randomized search. This heuristic, which we shall call RMAX, is based on ideas first suggested by Johri and Matula [14]. It has two user-definable parameters, *setlim* and *candnum*, and proceeds as follows: at any given time there is a set C (initially empty) of vertices in the current clique, and a set U consisting of all those remaining vertices that are adjacent to all members of C. If $|U| \leq$ *setlim*, the above branch-and-bound code (without the initial reordering) is invoked to find the maximum clique in U, and this is added to C. Otherwise, we sample *candnum* vertices and choose one with maximum degree (ties broken in favor of the earliest found). The chosen vertex is then added to C, U is updated, and we repeat. This whole randomized process can then itself be repeated (typically we did this 100–200 times) and the best clique found used as our lower bound. Our standard parameter settings were *setlim* = *candnum* = 100.

Here is a brief summary of the results of running the above algorithms on the graphs arising in this paper. The algorithms were run on an SGI Challenge computer with 100-Mhz MIPS R4400 processors.[13] Fig. 3 is based on a sample of four graphs for each number of users per cell, with the number of vertices ranging from 36 to 4320. For the largest of these, SLI took 18–23 s per run, and RMAX took about 3 s per run. (CMAX was not run.) We obtained matching

---

[13] SGI Challenge and MIPS are trademarks of Silicon Graphics, Inc.

upper and lower bounds for all graphs with less than 1000 vertices, and for all but four of the larger ones. For these four the lower and upper bounds were within 2.2% of each other. Such an empirically good match between bounds is a fortunate property of the classes of graphs considered. For randomly generated graphs (graphs in which each possible edge is present with probability .5, independently of all others), the expected value of $\chi(G)/\omega(G)$ goes to infinity as n increases. Note, however, that when a gap exists in our results it need not be because a true gap exists between $\omega(G)$ and $\chi(G)$. It might be that our coloring heuristics failed to find the best possible coloring, or our clique heuristic failed to find the biggest clique, or both. (When gaps occurred, we often attempted to find better colorings using tabu search and simulated annealing, but were successful in only one case, mentioned below.)

Fig. 4 is based on a sample of four graphs for each interference ratio, each graph having 3240 vertices. The upper and lower bounds matched on only one of these 28 graphs, although they never differed by more than 6%, with 3%–4% a more typical gap. The values for the fixed reuse patterns in this figure were checked using 800-vertex graphs. Here, there were gaps only for the radii $\alpha = 5$ and $\alpha = 6.5$. In both these cases we were able to run CMAX (it took about 1.3 s for each of these 800-vertex graphs). The best colorings found by SLI used 13 and 15 colors, respectively. In the case of $\alpha = 5$, however, we were able to find an 11 coloring using the simulated annealing algorithm of [21].

Fig. 5 is once again based on a sample of four graphs for each number of users per cell, with graphs sizes ranging from 33 to 3960 vertices. Upper and lower bounds matched on all but two of the graphs, both 3960-vertex graphs on which the gap was less than 1.1%. Fig. 6, which is based on a fixed gridlike distribution of mobiles, has just one graph per number of users, with sizes ranging from 52 vertices to 1976 over a total of 21 graphs. Upper and lower bounds matched on all but four of the graphs. The results in Fig. 8 are based on another set of 21 graphs with the same range of sizes. For most of these the upper and lower bounds do not match, but the gap is never more than 12%, and it was typically more like 5%.

APPENDIX B
OPTIMALITY OF THE SQUARE-ROOT POWER CONTROL

In this Appendix, we prove the optimality of the square-root power control strategy with and without shadow fading. More precisely, we prove that when the propagation loss is compensated by adding (in decibels) a fraction of the loss and fading, the optimal coefficient for such a compensation equals 0.5.

The definitions of distances are given in Fig. 2. Additionally, we denote by $P_F(A)$, where F and A equals $M_1, M_2, B_1,$ or B_2, the power from the mobile or the base F received at the mobile or the base A. The random variable Θ_{FA} represents the shadow fading between F and A, where F and A can be either a mobile or base station. Finally, κ is the propagation loss compensation constant.

We start by evaluating the power from the mobiles received at *their* base stations including the compensation factor[14]

$$P_{M_1}(B_1) = P_M \Theta_{M_1 B_1} \left(\frac{1}{\Theta_{M_1 B_1}} \right)^\kappa \tag{15}$$

$$P_{M_2}(B_2) = P_M \Theta_{M_2 B_2} \left(\frac{1}{\Theta_{M_2 B_2}} \right)^\kappa. \tag{16}$$

Similarly, we evaluate the power received at the base stations from *their* mobiles after compensation

$$P_{B_1}(M_1) = P_B \Theta_{M_1 B_1} \left(\frac{1}{\Theta_{M_1 B_1}} \right)^\kappa \tag{17}$$

$$P_{B_2}(M_2) = P_B \Theta_{M_2 B_2} \left(\frac{1}{\Theta_{M_2 B_2}} \right)^\kappa. \tag{18}$$

Now, we evaluate the interference level of mobiles at the other-than-their-own stations and of base stations at the other-than-their-own mobiles. Note that in these equations, the compensation is based on the signal path[15], while the fading is based on the interfering path[16]

$$P_{M_1}(B_2) = P_M \Theta_{M_1 B_2} \left(\frac{1}{\Theta_{M_1 B_1}} \right)^\kappa \tag{19}$$

$$P_{M_2}(B_1) = P_M \Theta_{M_2 B_1} \left(\frac{1}{\Theta_{M_2 B_2}} \right)^\kappa \tag{20}$$

$$P_{B_1}(M_2) = P_B \Theta_{M_2 B_1} \left(\frac{1}{\Theta_{M_1 B_1}} \right)^\kappa \tag{21}$$

$$P_{B_2}(M_1) = P_B \Theta_{M_1 B_2} \left(\frac{1}{\Theta_{M_2 B_2}} \right)^\kappa. \tag{22}$$

In order for the two mobiles to be compatible, the power levels must satisfy the following set of conditions:

$$P_{M_1}(B_1) \geq \alpha^r \cdot P_{M_2}(B_1) \tag{23}$$
$$P_{M_2}(B_2) \geq \alpha^r \cdot P_{M_1}(B_2) \tag{24}$$
$$P_{B_1}(M_1) \geq \alpha^r \cdot P_{B_2}(M_1) \tag{25}$$
$$P_{B_2}(M_2) \geq \alpha^r \cdot P_{B_1}(M_2). \tag{26}$$

Substituting (15) and (20) into the inequality (23) results in

$$P_M \Theta_{M_1 B_1} \left(\frac{1}{\Theta_{M_1 B_1}} \right)^\kappa \geq \alpha^r P_M \Theta_{M_2 B_1} \left(\frac{1}{\Theta_{M_2 B_2}} \right)^\kappa \tag{27}$$

which can be further rearranged to give

$$\alpha^r \Theta_{M_2 B_1} \leq \left(\Theta_{M_1 B_1} \right)^{1-\kappa} \left(\Theta_{M_2 B_2} \right)^\kappa. \tag{28}$$

Similarly, substituting (18) and (21) into the inequality (21) results in

$$P_B \Theta_{M_2 B_2} x_2^r \left(\frac{1}{\Theta_{M_2 B_2}} \right)^\kappa \geq \alpha^r P_B \Theta_{M_2 B_1} \left(\frac{1}{\Theta_{M_1 B_1}} \right)^\kappa \tag{29}$$

which after rearrangement yields

$$\alpha^r \Theta_{M_2 B_1} \leq \left(\Theta_{M_1 B_1} \right)^\kappa \left(\Theta_{M_2 B_2} \right)^{1-\kappa}. \tag{30}$$

---

[14] Note that, in practice, the compensation is done at the transmitting end by increasing the transmitted power based on the measurements at the receiving end.

[15] Path between a base station and its mobiles or between a mobile and its base station.

[16] For example, path between a base station and other-than-its-own mobiles.

In order to maximize the probability of the two mobiles being compatible, we need to maximize the minimum of the right-hand sides of inequalities (28) and (30) with respect to κ. I.e., we will attempt to find

$$\max_\kappa \{ \min[(\Theta_{M_1 B_1})^\kappa \cdot (\Theta_{M_2 B_2})^{1-\kappa}],$$
$$[(\Theta_{M_1 B_1})^{1-\kappa} \cdot (\Theta_{M_2 B_2})^\kappa] \}. \tag{31}$$

Since in (31) one term is an increasing while the other is a decreasing function of κ, the maximum of the minimum of the two terms occur when the two terms are equal. Thus

$$(\Theta_{M_1 B_1})^\kappa \cdot (\Theta_{M_2 B_2})^{1-\kappa} = (\Theta_{M_1 B_1})^{1-\kappa} \cdot (\Theta_{M_2 B_2})^\kappa \tag{32}$$

which, after some manipulations and for arbitrary $\Theta_{M_1 B_1}$, and $\Theta_{M_2 B_2}$, yields

$$\kappa = \frac{1}{2}. \tag{33}$$

Proceeding with the inequalities (24) and (25) in a similar manner yields the same optimal value for κ. The above proof assumed the presence of shadow fading. Substituting $\Theta_{XY} = x_i^{-r}$ for all X and Y, where x_i is the distance between X and Y, proves the optimality of $\kappa = 0.5$ for the no shadow-fading case.

ACKNOWLEDGMENT

REFERENCES

[1] V. H. MacDonald, "Advanced mobile phone system: The cellular concept," *Bell Syst. Tech. J.*, vol. 58, no. 1, pp. 15–41, Jan. 1979.
[2] S. Nanda and D. J. Goodman, "Dynamic resources acquisition: Distributed carrier allocation for TDMA cellular systems," in *Third Generation Wireless Information Networks*, S. Nanda and D. J. Goodman, Eds. Boston, MA: Kluwer, 1992.
[3] V. Prabhu and S. S. Rappaport, "Approximate analysis of dynamic channel assignment in large systems with cellular structure," *IEEE Trans. Commun.*, vol. COM-22, pp. 1715–1720, Oct. 1974.
[4] J. C.-I. Chuang, "Performance issues and algorithms for dynamic channel assignment," *IEEE J. Select. Areas Commun.*, vol. 11, no. 6, Aug. 1993.
[5] F. K. Hwang, P. E. Wright, and B. D. Lubachevsky, "Simple, effective, dynamic channel allocation for cellular systems," Internal AT&T Tech. Memo.
[6] J. Zander and H. Eriksson, "Asymptotic bounds on the performance of a class of dynamic channel assignment algorithms," *IEEE J. Select. Areas Commun.*, vol. 11, no. 6, pp. 926–933, Aug. 1993.
[7] W. C. Jakes Jr., Ed., *Microwave Mobile Communications*. New York: Wiley, 1974.
[8] T. J. Kahava and N. D. Georganas, "A hybrid channel assignment scheme in large-scale, cellular-structured mobile communication systems," *IEEE Trans. Commun.*, vol. COM-26, pp. 432–438, Apr. 1978.
[9] S. M. Elnoubi, R. Singh, and S. C. Gupta, "A new frequency channel assignment algorithm in high capacity mobile communication systems," *IEEE Trans. Veh. Technol.*, vol. VT-32, pp. 125–131, Aug. 1982.
[10] D. E. Everitt and N. W. Macfadyen, "Analysis of multicellular mobile radiotelephone systems with loss," *British Telecommun. Tech. J.*, vol. 1, no. 2, pp. 37–45, Oct. 1983.
[11] P.-A. Raymond, "Performance analysis of cellular networks," *IEEE Trans. Commun.*, vol. 39, Dec. 1991.
[12] "DECT services and facilities requirements specification," RES3S (3) 90, Rev. 5, May 4, 1990.
[13] M. R. Garey and D. S. Johnson, *Computers and Intractability: A Guide to the Theory of NP-Completeness*. New York: Freeman, 1979.

[14] A. Johri and D. W. Matula, "Probabilistic bounds and heuristic algorithms for coloring large random graphs," Southern Methodist Univ., Dallas, TX, Tech. Rep., 1982.

[15] M. Duque-Antón, D. Kunz, and B. Rüber, "Channel assignment for cellular radio using simulated annealing," *IEEE Trans. Veh. Technol.*, vol. 42, Feb. 1993.

[16] M. Duque-Antón and D. Kunz, "Channel assignment based on neural network algorithms," in *Proc. DMR IV*, Oslo, Norway, June 26–28, 1990, pp. 5.4.1–5.4.9.

[17] R. W. Nettleton and G. R. Schloemer, "A high-capacity assignment method for cellular mobile telephone systems," in *Proc. VTC'39*, pp. 359–367, May 1989.

[18] M. Serizawa and D. J. Goodman, "Instability and deadlock of distributed dynamic channel allocation," in *Proc. 1993 43rd IEEE Veh. Technol. Conf.*, Secaucus, NJ, May 18–20, 1993.

[19] J. F. Whitehead, "Performance and capacity of distributed dynamic channel assignment and power control in shadow fading," in *Proc. ICC'93*, Geneva, Switzerland, pp. 910–914, May 23–26, 1993.

[20] J. F. Whitehead, "Signal-level-based dynamic power control for co-channel interference management," in *Proc. VTC'93*, Secaucus, NJ, May 18–20, 1993.

[21] D. S. Johnson, C. R. Aragon, L. A. McGeoch, and C. Schevon, "Optimization by simulated annealing: An experimental evaluation-Part II, graph coloring and number partitioning," *Operations Res.*, vol. 39, pp. 378–406, 1991.

[22] R. Carraghan and P. Pardalos, "An exact algorithm for the maximum clique problem," *Operations Res. Lett.*, vol. 9, pp. 375–382, 1990.

[23] D. W. Matula, G. Marble, and J. D. Isaacson, "Graph coloring algorithms," in *Graph Theory and Computing*, R. C. Read, Ed. New York Academic, 1972, pp. 109–122.

[24] A. Hertz and D. de Werra, "Using tabu search techniques for graph coloring," *Computing*, vol. 39, pp. 345–351, 1987.

Jack H. Winters (S'77–M'81–SM'88–F'96) received the B.S.E.E. degree from the University of Cincinnati, OH, in 1977, and the M.S. and Ph.D. degrees in electrical engineering from Ohio State University, Columbus, in 1978 and 1981, respectively.

Since 1981 he has been with AT&T Bell Laboratories and now AT&T Laboratories—Research, where he is in the Wireless Systems Research Department. He has studied signal processing techniques for increasing the capacity and reducing signal distortion in fiber optic, mobile radio, and indoor radio systems, and is currently studying adaptive arrays and equalization for indoor and mobile radio.

David S. Johnson received the B.A. degree in mathematics from Amherst College, MA, in 1967, and the M.S. degree in 1968 and the Ph.D. degree in 1973, both in mathematics, from the Massachusetts Institute of Technology, Cambridge.

Since then he has worked for AT&T Bell Laboratories in its various incarnations, and is currently head of the Algorithms and Optimization Department at AT&T Laboratories, Murray Hill, NJ. His current research interests include the theory of NP-completeness and the theoretical and experimental analysis of algorithms, with special emphasis on graph coloring, bin packing, and the traveling salesman problem.

Zygmunt J. Haas (S'84–M'88–SM'90) received the B.Sc. degree in electrical engineering in 1979 and the M.Sc. degree in electrical engineering in 1985. In 1988, he received the Ph.D. degree from Stanford University, Stanford, CA

He subsequently joined AT&T Bell Laboratories in Holmdel, NJ, as a Member of Technical Staff in the Network Research Department. There he pursued research on wireless communications, mobility management, fast protocols, optical networks, and optical switching. From September 1994 to July 1995, he worked for the AT&T Wireless Center of Excellence in Whippany, NJ, where he investigated various aspects of wireless and mobile networking, concentrating on TCP/IP networks. In August 1995, he joined the faculty of the School of Electrical Engineering at Cornell University, Ithaca, NY, as Associate Professor. He is an author of numerous technical papers and holds 12 patents in the fields of high-speed networking, wireless networks, and optical switching. His interests include mobile and wireless communication and networks, personal communication service, and high-speed communication and protocols.

Dr. Haas has organized several Workshops, delivered tutorials at major IEEE conferences, and serves as Editor of several journals. He was a Guest Editor of two issues of the IEEE JOURNAL ON SELECTED AREAS IN COMMUNICATION ("Gigabit Networks" and "Mobile Computing Networks"). He is a Voting Member of ACM and the Secretary of the IEEE Technical Committee on Personal Communications.